THE ASTROPHYSICAL JOURNAL, 522:1079–1087, 1999 September 10

OPTIMAL EXCITATION OF MAGNETIC FIELDS

BRIAN F. FARRELL
Department for Earth and Planetary Sciences, Harvard University, Pierce Hall, 29 Oxford Street, Cambridge, MA 02138; farrell@io.harvard.edu
AND
PETROS J. IOANNOU
Section of Astronomy, Astrophysics, and Mechanics, Department of Physics, University of Athens, Panepistimiopolis, 15784 Zografos, Athens, Greece; pji@atlaa.uos.gr
Received 1998 July 20; accepted 1999 April 19

ABSTRACT

The mechanism by which large-scale magnetic fields in stars and galaxies arise remains uncertain, but it is believed that initially small internally generated or primordial seed fields are amplified and organized by motions in the conducting fluid interiors of these bodies. Methods for analyzing this process in the weak field limit are based on the induction equation and fall into two classes: those involving advection of the magnetic field as a passive tracer, and those involving calculation of exponential instabilities. The former is a nonmodal stability analysis, while the latter is essentially modal. In this work these two methods of analysis are synthesized, making use of recent advances in the theory of nonnormal system dynamics. An application of this generalized stability analysis to the helical dynamo model of Lortz is described in which the maximum field growth over prescribed time intervals and the perturbation structures producing this growth are identified.

Subject headings: hydrodynamics — instabilities — magnetic fields — MHD

1. INTRODUCTION

It is generally accepted that amplification of solar and galactic magnetic fields can be ascribed to magnetohydrodynamic (MHD) mechanisms that tap the kinetic energy of motions of the conductive fluid (Zeldovich, Ruzmaikin, & Sokoloff 1983). The induction equation governing generation of magnetic field by fluid motion in the weak field limit appropriate to solar and early stages of the development of Galactic fields is explicitly linear in the magnetic field $\boldsymbol{B}$ and can be written in the nondimensional form

$$\frac{\partial \boldsymbol{B}}{\partial t} = \boldsymbol{\nabla} \wedge (\boldsymbol{v} \wedge \boldsymbol{B}) + \frac{1}{R_m} \boldsymbol{\nabla}^2 \boldsymbol{B} , \tag{1}$$

$$\boldsymbol{\nabla} \cdot \boldsymbol{B} = 0 , \tag{2}$$

where $\boldsymbol{v}$ is the advecting velocity field and $R_m = UL/\eta$ is the magnetic Reynolds number. In the definition of R_m the magnetic diffusivity $\eta = \mu_0 \sigma$ has been used, where μ_0 is the magnetic permeability of free space and σ is the electrical conductivity of the medium. Characteristic scales for the spatial extent of the domain, L, and for the velocity of the mean motion, U, have also been assumed. Boundary conditions on the velocity field are implicit in its specification, while boundary conditions on the magnetic field are usually chosen to correspond either to an idealized insulator, in which case $\boldsymbol{B}$ is continued into a potential field in the insulating region, or to a perfect conductor, in which case both the normal component of the magnetic field and the tangential component of the current are required to vanish.

A traditional procedure used to study field amplification governed by equation (1) given a domain and a velocity field is to assume modal solutions of the form $\boldsymbol{B} = \hat{\boldsymbol{B}} e^{\sigma t}$ so that equation (1) becomes an eigenproblem with complex eigenfrequencies σ implying exponential growth of $\boldsymbol{B}$ at the rate of Re σ:

$$\sigma \boldsymbol{B} = \boldsymbol{\nabla} \wedge (\boldsymbol{v} \wedge \boldsymbol{B}) + \frac{1}{R_m} \boldsymbol{\nabla}^2 \boldsymbol{B} . \tag{3}$$

Historically, demonstrating the existence of unstable eigenmodes was thought important for establishing the possibility of field growth in light of the antidynamo result of Cowling (1934). The eigenproblem approach has served this purpose with a number of unstable flows having been identified (Gubbins 1973; Pekeris, Accad, & Shkoller 1973). These results demonstrate modal instability of the induction equation implying asymptotic growth in the limit $t \to \infty$. For examples such as the α^2 dynamo (Moffatt 1978) in which the induction equation has a complete set of orthogonal eigenfunctions, the eigenspectrum exhausts the possibilities for perturbation growth so that the boundary in R_m separating regions of Re $\sigma > 0$ from those with Re $\sigma < 0$ also separates regions in which all perturbations decay from regions in which at least one perturbation grows. Because the induction equation does not in general have orthogonal eigenvectors, there is the possibility for perturbation growth even in cases for which all eigenvalues of equation (2) have Re $\sigma < 0$.

Recognition of the importance of the analogous nonmodal perturbation growth processes in fluid mechanics goes back to the work of Kelvin (1887) and Orr (1907) and has been studied in connection with the formation of cyclones (Farrell 1982, 1984, 1989) and transition to turbulence (Farrell 1988; Butler & Farrell 1992; Gustavsson 1991; Reddy & Henningson 1993; Farrell & Ioannou 1993a; Trefethen et al. 1993). While the possibility of nonmodal growth in the induction equation was described by Moffatt (1978) among others, and has been discussed in an astrophysical context (Childress & Gilbert 1995; Howard & Kulsrud 1997), systematic application of nonmodal analysis to this equation has not heretofore been presented. We choose as an example problem the helical dynamo flow (Ruzmaikin, Sokoloff, & Shukurov 1988; Gilbert 1988) because it has been widely studied and many results relating to its stability are available. We believe the results we present below are generic to shear flows in conducting fluids and that attempting to model more precisely a stellar or

galactic flow, which is in any case uncertain, is unwarranted at this point. With this assumed flow the induction equation is highly nonnormal, and transient growth of $\boldsymbol{B}$ occurs for parameter values for which only decaying eigenmodes exist. We find that transient perturbation growth increases as $R_m \to \infty$, in agreement with intuition, rather than decreasing with R_m as does max (Re σ), the growth rate of the most unstable eigenmode. This increase of transient field growth with R_m that is characteristic of nonnormal dynamics is important for physical systems such as stellar interiors where high magnetic Reynolds number $O(10^{10})$ make the slow exponential growth predicted by modal analysis unlikely to be physically relevant.

In addition to application to field growth in flows that are assumed to be steady, as in our example problem, analysis of transient nonnormal growth processes is also applicable to advancing theoretical understanding of magnetic fields that emerge in flows which are time dependent and aperiodic, where traditional modal analysis with its assumption of temporal homogeneity is not directly applicable. Efforts to understand field growth and maintenance in time-dependent systems has been based on two approaches: mean field theory, such as the α dynamo (Krause & Rädler 1980; Braginskii 1965a, 1965b; Hoyng 1992), on the one hand, and stochastic models (Hoyng 1987a, 1987b, 1988; Farrell & Ioannou 1999a), on the other. These approaches employ a separation between a resolved field and an unresolved field, while nonmodal analysis can be used to study field growth in time-dependent systems without requiring separation between resolved and unresolved scales (Farrell & Ioannou 1996b, 1999b).

We first review the methods to be used in § 2 and then apply them to our simple model example in § 3.

2. GENERALIZED STABILITY ANALYSIS OF NONNORMAL SYSTEMS

Generalized stability analysis provides methods for studying transient growth processes occurring in nonnormal dynamical systems (cf. Farrell & Ioannou 1996a). The system we wish to analyze is the induction equation (1) together with its boundary conditions, which can be written in the general dynamical system form

$$\frac{dB}{dt} = \boldsymbol{A}B \,, \tag{4}$$

where $\boldsymbol{A}$ is the linear induction operator, which we will approximate as a finite-dimensional matrix and B is the column vector of the components of the magnetic field. For our purposes the crucial characteristic of this dynamical system matrix is its degree of normality. A normal matrix, defined as a matrix for which the commutator $\boldsymbol{A}\boldsymbol{A}^\dagger - \boldsymbol{A}^\dagger\boldsymbol{A}$ vanishes, has orthogonal eigenvectors, and its stability is determined solely by the growth rates of these eigenvectors.[1] If the commutator $\boldsymbol{A}\boldsymbol{A}^\dagger - \boldsymbol{A}^\dagger\boldsymbol{A} \neq \boldsymbol{0}$, at least some of the eigenvectors of $\boldsymbol{A}$ are not orthogonal and stability cannot be deduced solely from the spectrum of $\boldsymbol{A}$. Instead a complete stability analysis proceeds from the solution of equation (4) for the propagator $\boldsymbol{\Phi}_{[t,0]}$:

$$B(t) = \boldsymbol{\Phi}_{[t,0]}B(0) \,, \tag{5}$$

after which calculation of the spectral norm of the propagator $\| \boldsymbol{\Phi}_{[t,0]} \|$ gives the maximum magnetic field growth at time t.[2]

Maximum instantaneous growth rate at any time t is obtained as the $t \to 0$ limit of a Taylor expansion of the propagator. This maximum instantaneous growth rate at time t is the greatest eigenvalue of the normal operator $(\boldsymbol{A}^\dagger + \boldsymbol{A})/2$, where $\boldsymbol{A}$ is the operator at time t. The corresponding eigenfunction is the field structure of maximum instantaneous growth rate. In general, for nonnormal $\boldsymbol{A}$ both the instantaneous growth rate and the corresponding structure differ from the most unstable eigenvalue of $\boldsymbol{A}$ and its corresponding eigenfunction.

Magnetic field growth at arbitrary time t is determined by singular value decomposition (SVD) of the propagator:

$$\boldsymbol{\Phi}_{[t,0]} = \boldsymbol{U}\boldsymbol{S}\boldsymbol{V}^\dagger \,, \tag{6}$$

in which $\boldsymbol{U}$ and $\boldsymbol{V}$ are unitary and $\boldsymbol{S}$ is diagonal with positive elements, each equal to growth at time t of the initial perturbation specified by the corresponding column of $\boldsymbol{V}$. The unitary matrix $\boldsymbol{V}$ has column vectors $\boldsymbol{v}_i$ that span the state space of the perturbations at the initial time, here taken to be $t = 0$. Each of the $\boldsymbol{v}_i$, is mapped with increase in amplitude S_{ii} into its associated $\boldsymbol{u}_i$. These orthogonal column vectors comprising $\boldsymbol{U}$ span the state space at time t.

The analogous eigenanalysis is

$$\boldsymbol{\Phi}_{[t,0]} = \boldsymbol{E}\boldsymbol{S}\boldsymbol{E}^{-1} \,, \tag{7}$$

in which $\boldsymbol{E}$ is the matrix of eigenvectors of $\boldsymbol{A}$ arranged in columns and λ is the diagonal matrix with $\lambda_{ii} = e^{p_i t}$, which provides information on the growth rate and structure of perturbations only in the limit $t \to \infty$. It is easily shown that $\max_i \boldsymbol{S}_{ii} \geq \max_i \mathrm{Re}\ \lambda_{ii}$ with equality only when $\boldsymbol{E} = \boldsymbol{U}$, which in turn implies that $\boldsymbol{A}$ in equation (2) is a normal matrix.

The goal of generalized stability analysis is to determine the perturbation growth potential for all times, and for this purpose analysis of the propagator of the dynamical system as outlined above is necessary for nonnormal systems such as that in equation (1).

3. GENERALIZED STABILITY ANALYSIS APPLIED TO THE HELICAL DYNAMO

3.1. *Formulation*

We will use as an example problem a helical dynamo (Gilbert 1988; Ruzmaikin et al. 1988) with axially symmetric velocities in the radial (r), azimuthal (θ), and axial (z) direction:

$$U_r = 0 \,, \quad U_\theta = U_0 r\Omega(r) = U_0 r e^{-r^2} \,, \quad U_z = U_0 e^{-r^2} \,. \tag{8}$$

The flow is contained in a cylinder with inner radius $r_1 = 0.5$ and outer radius $r_2 = 1$. The inner cylinder boundary, r_1, will be assumed bounded by a perfect electrical conductor, while the outer boundary at r_2 will be assumed bounded either by a perfect conductor or by an insulator.

Magnetic field perturbations:

$$B_r = \hat{B}_r(t, r)e^{ikz + im\theta} \,, \quad B_\theta = \hat{B}_\theta(t, r)e^{ikz + im\theta} \,,$$
$$B_z = \hat{B}_z(t, r)e^{ikz + im\theta} \tag{9}$$

[1] Here $\boldsymbol{A}^\dagger$ denotes the adjoint matrix defined for the inner product $(\cdot, \cdot)$ by $(\boldsymbol{A}^\dagger B, B) = (B, \boldsymbol{A}B)$. In the Euclidean norm the adjoint matrix is the Hermitian transpose of $\boldsymbol{A}$.

[2] If $\boldsymbol{A}$ is autonomous the propagator can be written explicitly as a matrix exponential: $\boldsymbol{\Phi}_{[t,0]} = e^{\boldsymbol{A}t}$.

evolve in time according to the induction equation:

$$\frac{d\hat{B}_r}{dt} = -i(m\Omega + kU_z)\hat{B}_r + \frac{1}{R_m}\left(L\hat{B}_r - \frac{2im}{r^2}\hat{B}_\theta\right), \quad (10)$$

$$\frac{d\hat{B}_\theta}{dt} = -i(m\Omega + kU_z)\hat{B}_\theta + r\frac{d\Omega}{dr}\hat{B}_r + \frac{1}{R_m}\left(L\hat{B}_\theta + \frac{2im}{r^2}\hat{B}_r\right), \quad (11)$$

$$\frac{d\hat{B}_z}{dt} = -i(m\Omega + kU_z)\hat{B}_z + \frac{dU_z}{dr}\hat{B}_r + \frac{1}{R_m}\left(L + \frac{1}{r^2}\right)\hat{B}_z, \quad (12)$$

in which appears the diffusion operator in cylindrical polar coordinates:

$$L = \frac{1}{r}\frac{d}{dr}\left(r\frac{d}{dr}\right) - \frac{m^2+1}{r^2} - k^2. \quad (13)$$

The radial and azimuthal magnetic field equations (10) and (11) decouple from the axial equation (12) and can be solved independently. The axial magnetic field simultaneously satisfies equation (12) while maintaining nondivergence of the magnetic field:

$$\frac{1}{r}\frac{d(rB_r)}{dr} + i\frac{m}{r}B_\theta + ikB_z = 0. \quad (14)$$

The magnetic Reynolds number, $R_m = U_0 L/\eta$, is defined in terms of the length scale $L = r_2 - r_1$, the velocity scale U_0, and the magnetic diffusivity $\eta = \mu_0\sigma$, where μ_0 is the magnetic permeability of free space and σ is the electrical conductivity of the material. Time is nondimensionalized by the advective timescale L/U_0. The differential operators are discretized to obtain a finite-dimensional dynamical system, and convergence is verified by doubling resolution [it was determined in this way that $O(R_m^{1/3})$ grid points are required for convergence of the discretized operator].

3.2. *Modal Analysis and Asymptotic Stability of the Induction Operator*

Asymptotic stability or instability of the induction equation is deduced by examining the temporal eigenvalues of equations (10) and (11). Diffusive coupling between the radial and azimuthal magnetic field components supports modal instability only for a restricted range of wavenumbers k, m. For the continuous flows considered here this dynamo has been demonstrated to be slow, i.e., the growth rate vanishes as $R_m \to \infty$, with maximum instability occurring for $m = -k$, under which condition it was shown by Ruzmaikin et al. (1988) that the growth rate decreases with Reynolds number as

$$\mathrm{Re}\,\sigma \approx \frac{1.4}{R_m^{1/2}} - \frac{3.7}{R_m^{3/4}}. \quad (15)$$

Application of Cowling's theorem (Cowling 1934) ensures that no unstable mode is supported in the physically interesting case of axisymmetric magnetic field perturbations ($m = 0$). In addition, for axial and azimuthal wavenumbers sufficiently far from the condition $m = -k$ for maximum instability, the spectrum is also stable for all Reynolds numbers. The growth rate of the most unstable mode is shown in Figure 1 for the annular flow (eq. [8]) with insulating boundary conditions at $r_2 = 1$ and conducting boundary conditions at $r_1 = 0.5$, for azimuthal wavenumber $m = 1$ and for both axial wavenumbers $k = -0.6$ and $k = -1$; in the same figure the asymptotic expression in equation (15) is plotted, showing that it captures the behavior of the growth rate as $R_m \to \infty$. The asymptotic expression in equation (15) does not apply to axisymmetric perturbations, which are found to decay as $R_m^{-1/3}$.

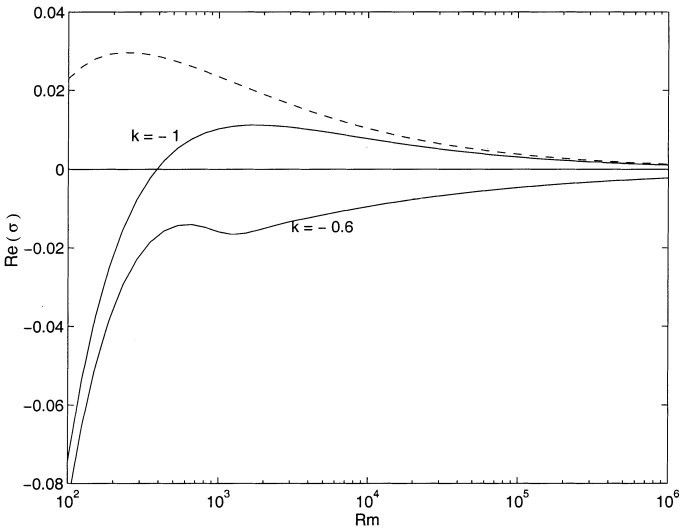

FIG. 1.—Growth rate of the most unstable mode as a function of Reynolds number, R_m, for $m = 1$ and $k = -0.6$, -1. The flow is confined to the region $0.5 < r < 1$, and the boundary conditions are conducting at the inner wall and insulating at the outer wall. The dashed curve shows the asymptotically valid prediction (eq. [15]) for the most unstable growth rate for $m = 1$ and $k = -1$.

The magnetic field associated with the least damped mode for the case $m = 1$, $k = -0.6$ at $R_m = 10^4$ is shown in Figure 2. The magnetic field of the least damped mode is concentrated in a boundary layer of thickness $O(R_m^{1/3})$ as expected from field expulsion arguments (Moffatt 1978).

Nonnormality of the induction operator implies that the initial magnetic perturbation that optimally excites the least damped mode is not the least damped mode itself but its biorthogonal, which is given by the corresponding least stable mode of the adjoint operator in the inner product corresponding to the mean magnetic energy density:

$$E = \frac{1}{\mu_0(r_2^2 - r_1^2)}\int_{r_1}^{r_2} r\,dr(|\hat{B}_r|^2 + |\hat{B}_\theta|^2 + |\hat{B}_z|^2). \quad (16)$$

In Figure 3 the three components of the adjoint mode corresponding to the least damped mode are plotted from which it can be seen that this adjoint mode extends throughout the flow rather than being concentrated at one boundary as was the case for the corresponding mode in Figure 2. In Figure 4 the time evolution of the energy of the initial condition consisting of this adjoint mode of the least damped mode is contrasted with the time evolution of the energy of the most unstable mode initial condition. Magnetic field intensification through stretching produces nearly linear growth for a time period $O(R_m^{1/3})$. After

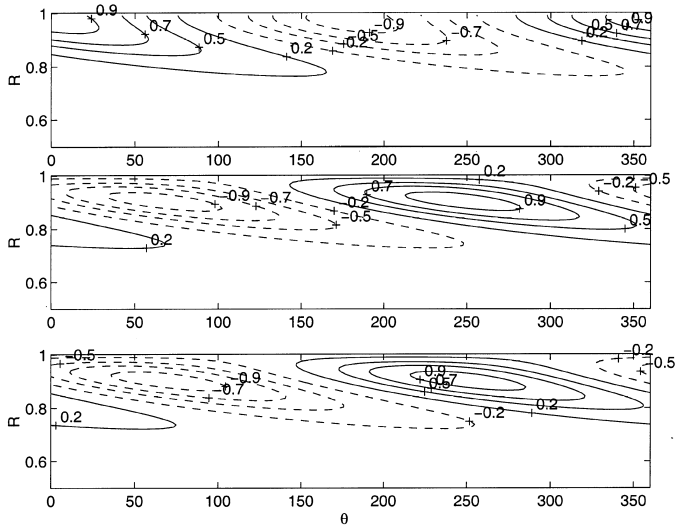

FIG. 2.—Cross section plots of the radial magnetic field B_r (*top panel*), the azimuthal magnetic field B_θ (*middle panel*), and the axial magnetic field B_z (*bottom panel*) in the $z = 0$ plane for the least stable mode at $R_m = 10^4$ with azimuthal and axial wavenumbers $m = 1$, $k = -0.6$. The magnetic field satisfies boundary conditions appropriate for a conducting inner wall and an insulating outer wall.

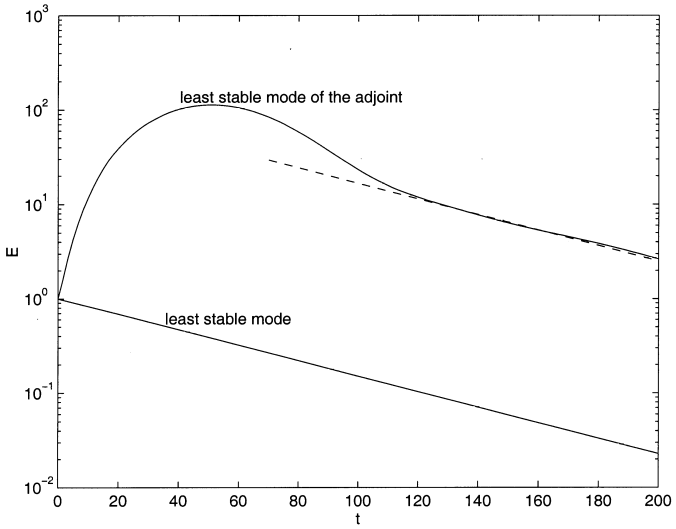

FIG. 4.—Comparison of the energy evolution of an initial perturbation in the form of the least stable mode and its adjoint mode at $R_m = 10^4$, $m = 1$, and $B = -0.6$. The adjoint mode can be shown to optimally excite the mode. After a period of transient growth the adjoint mode initial condition assumes the form of the mode (at $t \approx 120$ in this graph). The asymptotic ratio of the energies of the least damped mode for these contrasting initial conditions is approximately 115.

this interval of linear growth the perturbation assumes the form of the most unstable mode but with much enhanced amplitude. It can be shown that the energy amplification factor achieved in the excitation of the most unstable mode by its adjoint mode is inversely proportional to the square of the energy inner product between the mode and its adjoint mode (Farrell & Ioannou 1996a), which for this problem is found to increase with Reynolds number as $R_m^{1/2}$.

The significance of the modes of a nonnormal system is not so much that the least damped mode asymptotically dominates the perturbation structure at large time, but rather that the modes serve as repositories for energy converted through kinematic deformation from kinetic to magnetic form. We have seen above an example of this process in the optimal excitation of the least damped mode by its adjoint. A similar situation is shown in Figure 5 for the unstable case with $m = 1$ and $k = -1$ and for $R_m = 10^3$ and $R_m = 10^5$. In this figure the energy growth of the fastest growing mode initial condition (*dashed lines*) is shown to always underestimate the optimal growth. It is clear that even though the mode dominates the structure after a time

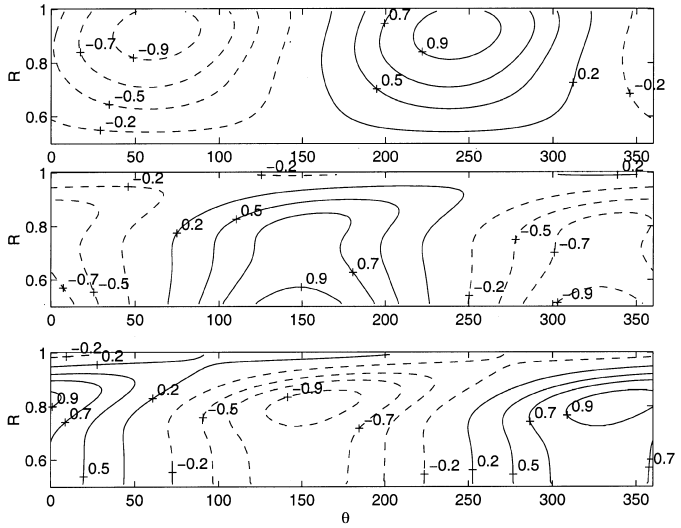

FIG. 3.—Radial magnetic field B_r (*top panel*), the azimuthal magnetic field B_θ (*middle panel*), and the axial magnetic field B_z (*bottom panel*) in the $z = 0$ plane for the adjoint mode in the energy metric corresponding to the least stable mode at $R_m = 10^4$ with aximuthal and axial wavenumbers $m = 1$, $k = -0.6$. The boundary conditions are conducting at the inner wall and insulating at the outer wall. This adjoint mode is the initial perturbation with unit energy that excites optimally the least stable mode.

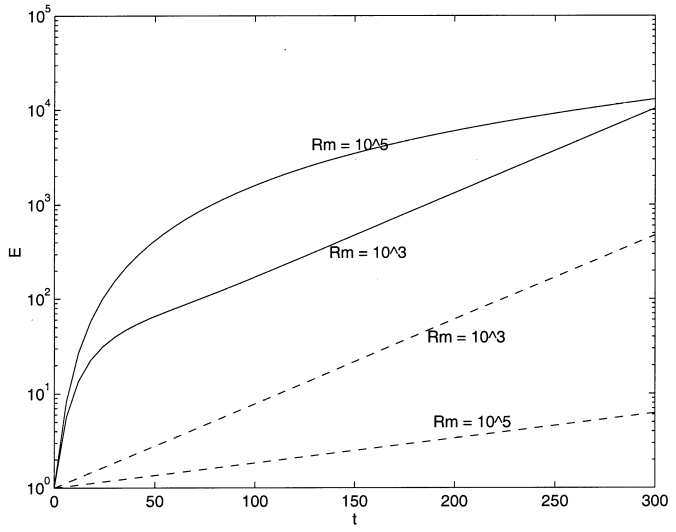

FIG. 5.—Modal energy growth (*dashed lines*) compared with optimal energy growth as a function of optimizing time for magnetic perturbations with azimuthal and axial wavenumbers $m = 1$ and $k = -1$ and for magnetic Reynolds numbers $R_m = 10^3$ and $R_m = 10^5$.

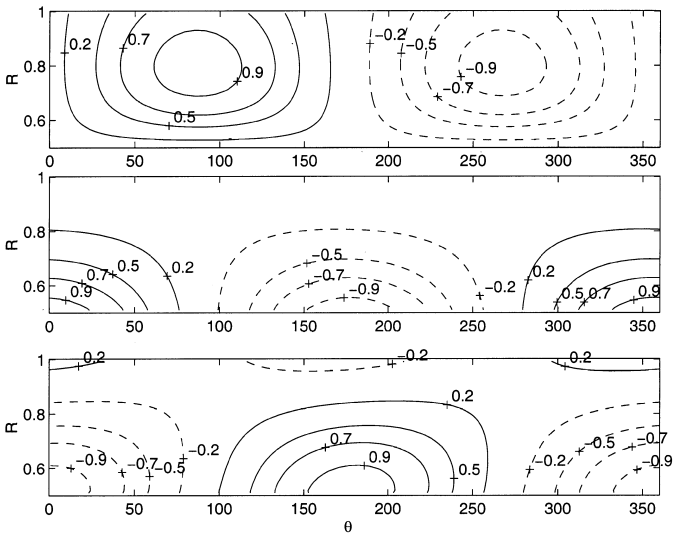

FIG. 6a

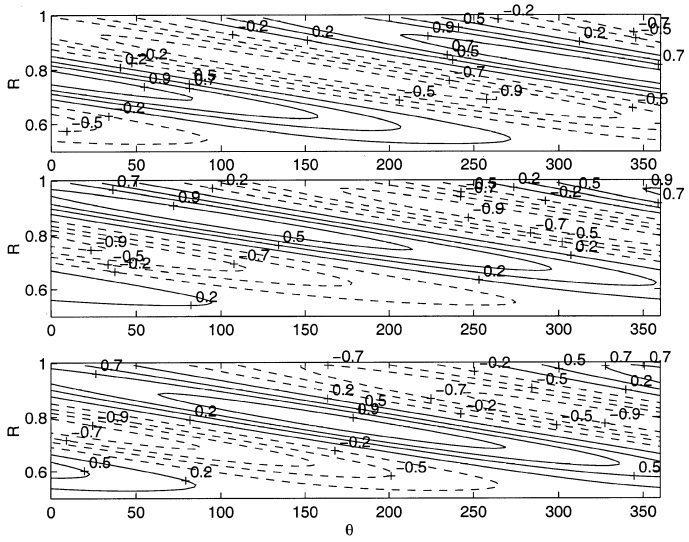

FIG. 6b

FIG. 6.—(*a*) Radial magnetic field B_r (*top panel*), azimuthal magnetic field B_θ (*middle panel*), and axial magnetic field B_z (*bottom panel*) in the $z = 0$ plane for the inviscid optimal perturbation that achieves the greatest energy growth at $t = 50$. Shown here is the optimal perturbation at $t = 0$. The dynamics are inviscid, and the azimuthal and axial wavenumbers are $m = 1$, $k = -0.6$. (*b*) The inviscid optimal perturbation evolved forward to the time of optimization $t = 50$. The energy has grown by a factor of 379.

$O(R_m^{1/3})$, other initial conditions result in far more effective excitation of the mode than does an initial condition consisting of the mode itself.

3.3. *Initial Magnetic Field Growth*

The initial field growth process for sufficiently high R_m is well described by the inviscid problem obtained from the $R_m \to \infty$ limit of the induction equations (10), (11), and (12), which can be integrated immediately to yield the magnetic field in terms of its initial state:

$$\hat{B}_r(r, t) = e^{-L_{ad}(r)t}\hat{B}_r(r, 0)\,, \tag{17}$$

$$\hat{B}_\theta(r, t) = e^{-L_{ad}(r)t}\hat{B}_\theta(r, 0) + r\frac{d\Omega}{dr}te^{-L_{ad}(r)t}\hat{B}_r(r, 0)\,, \tag{18}$$

$$\hat{B}_z(r, t) = e^{-L_{ad}(r)t}\hat{B}_z(r, 0) + \frac{dU_z}{dr}te^{-L_{ad}(r)t}\hat{B}_r(r, 0)\,, \tag{19}$$

with $L_{ad}(r) = i(m\Omega + kU_z)$ the advection operator. The linear growth of $\hat{B}_\theta$ and $\hat{B}_z$ under shearing by the background flow as revealed by equations (18) and (19) implies quadratic magnetic energy growth. This field stretching process can be seen in Figure 6*a*, where the $t = 50$ optimal initial perturbation (the initial condition that maximizes magnetic energy growth at time $t = 50$) is seen to be stretched to ever finer scales as time proceeds (cf. Fig. 6*b*). In the inviscid case this stretching continues unopposed, producing ever finer magnetic field structure; in contrast, for flows with any finite value of magnetic Reynolds number, an initial field asymptotically approaches the fixed structure of the least damped mode.

Comparing the viscous solutions of equations (10)–(12) with the inviscid solutions in equations (17)–(19), we find that the inviscid solution remains valid until the integrated effect of diffusion becomes $O(1)$ at $t = O(R_m^{1/3})$, in agreement with Parker's (1963) estimate. This is a consequence of diffusion in shearing flows leading to decay of the field at an exponential rate which increases as t^3 (Tung 1983; Farrell & Ioannou 1993a; refer to the Appendix for details).

3.4. *Optimal Field Growth*

In order to enforce nondivergence of the magnetic field in the initial-value problem, we follow Lortz (1968) in expressing the field in helical coordinates using two scalar functions $f = \hat{f}(r, t)e^{i\psi}$ and $F = \hat{F}(r, t)e^{i\psi}$ with $\psi = m\theta + kz$. In terms of these functions the field is

$$\boldsymbol{B} = f\boldsymbol{h} + \boldsymbol{h} \wedge \nabla F\,, \tag{20}$$

with the helical vector $\boldsymbol{h}$ defined as

$$\boldsymbol{h} = \frac{r}{q}\nabla r \wedge \nabla\psi\,, \tag{21}$$

and $q = m^2 + k^2r^2$. The field components are

$$\hat{B}_r = -i\frac{\hat{F}}{r}\,, \tag{22}$$

$$\hat{B}_\theta = -\frac{kr}{q}\hat{f} + \frac{m}{q}\frac{d\hat{F}}{dr}\,, \tag{23}$$

$$\hat{B}_z = \frac{m}{q}\hat{f} + \frac{kr}{q}\frac{d\hat{F}}{dr}\,, \tag{24}$$

for which it can be easily verified that $\nabla \cdot \boldsymbol{B} = 0$.

The evolution of the magnetic field is obtained from integration of the dynamical system:

$$\frac{d}{dt}\begin{pmatrix}\hat{F}\\ \hat{f}\end{pmatrix} = T\begin{pmatrix}\hat{F}\\ \hat{f}\end{pmatrix}\,, \tag{25}$$

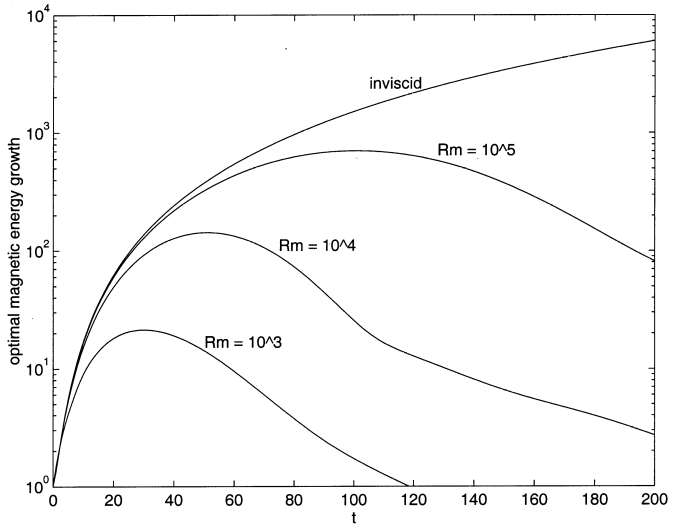

FIG. 7a

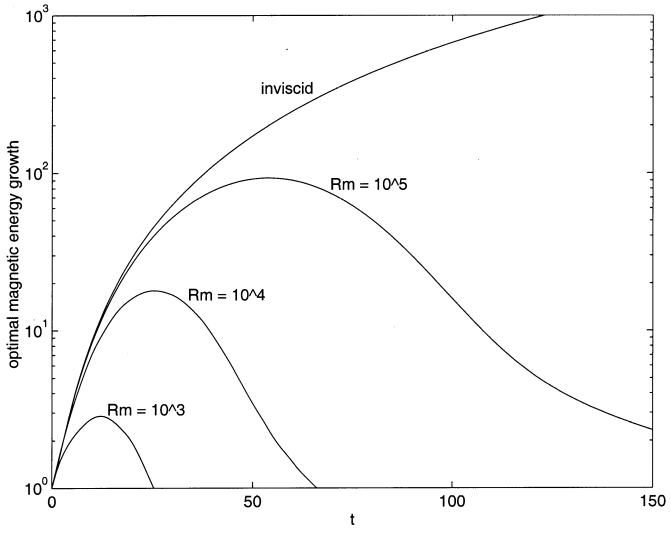

FIG. 7b

FIG. 7.—Optimal energy growth as a function of optimizing time for magnetic perturbations with azimuthal and axial wavenumbers $m = 1$ and $k = -0.6$ for Reynolds numbers $R_m = 10^3$, $R_m = 10^4$, $R_m = 10^5$, as well as for the inviscid case. (*b*) Optimal energy growth as a function of optimizing time for axisymmetric magnetic perturbations with azimuthal and axial wavenumbers $m = 0$ and $k = -1$ for Reynolds numbers $R_m = 10^3$, $R_m = 10^4$, $R_m = 10^5$ as well as for the inviscid case.

with dynamical operator

$$\boldsymbol{T} = \begin{pmatrix} A & B \\ C & D \end{pmatrix}, \tag{26}$$

where

$$\begin{aligned} A &= -L_{\rm ad} + \frac{1}{R_m}\left(L + \frac{1}{r^2} - \frac{2k^2 r}{q}\frac{d}{dr}\right), \\ B &= -\frac{2}{R_m}\frac{mk}{q}, \\ C &= -i\frac{m}{r}\frac{dU_z}{dr} + ikr\frac{d\Omega}{dr} \\ &\quad + \frac{1}{R_m}\left[-\frac{2mk}{r^2} + \left(\frac{2mk}{rq} - \frac{4mk^3 r}{q}\right)\frac{d}{dr} + \frac{2mk}{q}\frac{d^2}{dr^2}\right], \\ D &= -L_{\rm ad} + \frac{1}{R_m}\left(\frac{m^2 - 3k^2r^2}{r^2 q} + \frac{4k^4 r^2}{q^2} - \frac{2k^2 r}{q}\frac{d}{dr} + L\right), \end{aligned} \tag{27}$$

in which $L_{\rm ad} = i(m\Omega + kU_z)$ is the advection operator and L is the diffusion operator (eq. [13]).

The boundary conditions are

$$\hat{F} = 0\,, \quad \frac{d\hat{f}}{dr} = 0 \tag{28}$$

at a conducting boundary, while at the insulating boundary at $r = 1$,

$$\hat{f} = 0\,, \quad \frac{d\hat{F}}{dr} = \frac{m^2 + k^2}{|k|}\frac{K_m(|k|)}{K_m'(|k|)}\hat{F}\,, \tag{29}$$

with K_m the modified Bessel function and K_m' its derivative.

Because we are concerned with the growth of magnetic field energy, it is advantageous to define a new generalized variable:

$$z = \boldsymbol{M}^{1/2}\begin{pmatrix} \hat{F} \\ \hat{f} \end{pmatrix}, \tag{30}$$

where $\boldsymbol{M}$ is the positive definite Hermitian matrix defining the inner product of the magnetic field energy density,

$$E = z^\dagger z = \begin{pmatrix} \hat{F} \\ \hat{f} \end{pmatrix}^\dagger \boldsymbol{M}\begin{pmatrix} \hat{F} \\ \hat{f} \end{pmatrix}. \tag{31}$$

This energy metric is given by

$$\boldsymbol{M} = \frac{2}{\mu_0(r_2^2 - r_1^2)}\begin{pmatrix} \dfrac{1}{r} + \left[\dfrac{r}{q}\dfrac{d}{dr}\right]^\dagger \dfrac{d}{dr} & 0 \\ 0 & \dfrac{r}{q} \end{pmatrix}, \tag{32}$$

where $[(r/q)\,d/dr]^\dagger$ denotes the operator adjoint to $(r/q)\,d/dr$ in the inner product: $(\hat{F}, \hat{F}) = \int_{r_1}^{r_2} dr\, \hat{F}^\dagger \hat{F}$ with appropriate boundary conditions imposed on $\hat{F}$.

The optimal energy growth that can be attained at t is given by the square of the spectral norm of the propagator, $\|\exp(\boldsymbol{M}^{1/2}\boldsymbol{T}\boldsymbol{M}^{-1/2}t)\|$, and the perturbation that produces this optimal growth, which we refer to as the optimal perturbation, can be found from an SVD decomposition of the propagator, as described in § 2. We have seen in Figure 5 the optimal growth as a function of optimizing time obtained for azimuthal wavenumber $m = 1$ and axial wavenumber $k = -1$ and Reynolds number $R_m = 10^3$, 10^5, for which parameters the induction equation is exponentially unstable. The growth revealed in Figure 5 substantially exceeds the exponential growth of the most unstable mode initial condition. By contrast, in Figure 7*a* the optimal growth is shown as a function of optimizing time for $m = 1$ and $k = -0.6$ and $R_m = 10^3$, 10^4, 10^5, all of which are asymptotically stable cases. The optimal growth for the inviscid case, which is also shown in Figure 7*a* reveals the expected quadratic energy growth with time and provides

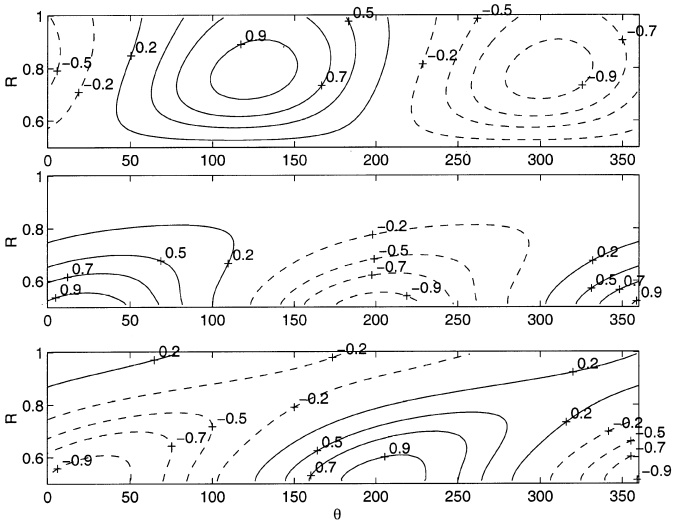

FIG. 8*a*

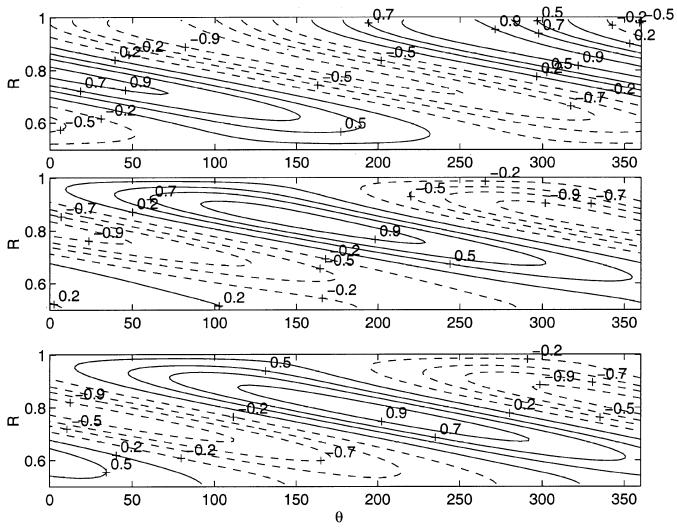

FIG. 8*b*

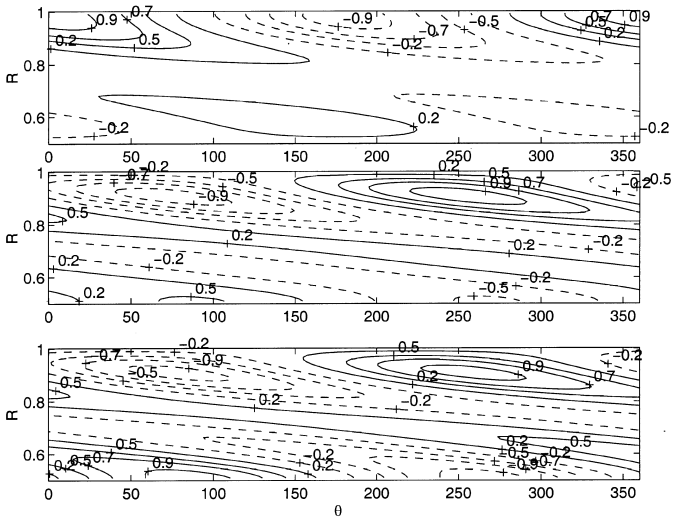

FIG. 8*c*

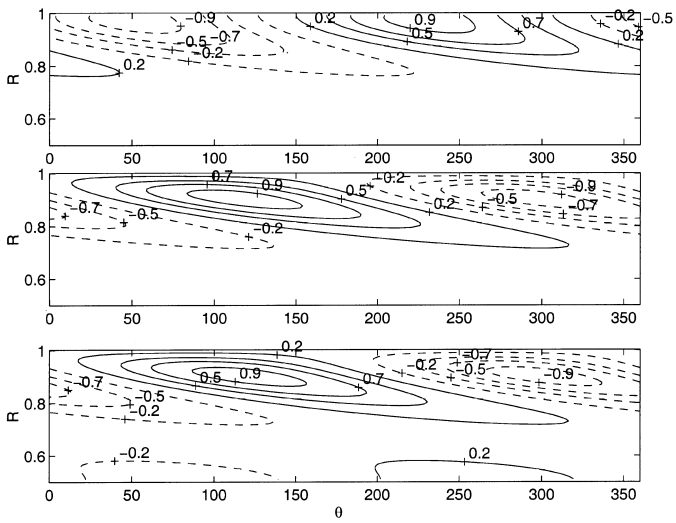

FIG. 8*d*

FIG. 8.—Radial magnetic field B_r (*top panel*), azimuthal magnetic field B_θ (*middle panel*) and axial magnetic field B_z (*bottom panel*) in the $z = 0$ plane for the optimal perturbation at Reynolds number $R_m = 10^4$ that achieves the greatest energy growth at $t = 50$. Shown here is the optimal perturbation at $t = 0$. The azimuthal and axial wavenumbers are $m = 1$, $k = -0.6$. (*b*) Optimal perturbation evolved forward to the time of optimization $t = 50$. The energy has grown by a factor of 142. (*c*) Optimal perturbation evolved forward to time $t = 100$. $E = 21.71$. (*d*) Optimal perturbation evolved forward to time $t = 200$. The perturbation has assumed modal form. $E = 2.132$.

an upper bound for perturbation growth for all magnetic Reynolds numbers. Examination of Figure 7 verifies that for $t < O(R_m^{1/3})$ the energy growth of stable and unstable cases are nearly identical, in accord with the arguments given in § 3.3.

The axisymmetric case is especially interesting physically, as observed magnetic fields are approximately axially symmetric. Cowling's theorem precludes the existence of exponentially growing modes in an axisymmetric velocity field so that nonmodal growth may be particularly relevant in explaining the existence of axial dipole fields. The optimal growth for $m = 0$ and $k = -1$ plotted as a function of optimizing time in Figure 7*b* shows robust transient growth which becomes unbounded as $R_m \to \infty$.

The temporal evolution of the perturbation producing optimal growth at $t = 50$ for $m = 1$, $k = -0.6$ is shown in Figures 8*a*, 8*b*, 8*c*, and 8*d*. At first the evolution parallels that of the inviscid case (cf. Fig. 6*b*), then diffusive effects become apparent by $t = 100$, and finally the structure assumes its asymptotic form as the least stable eigenmode (cf. Fig. 8*d* and Fig. 2).

In asymptotically stable nonnormal systems a characteristic measure of stability is the maximum possible energy growth. This maximum energy growth for the problem at hand is a function of wavenumber and R_m. The time of maximum growth scales as $R_m^{1/3}$ (refer to Fig. 9), and the maximum magnetic energy scales as $R_m^{2/3}$. This is verified in Figure 10, in which the maximum magnetic energy growth is plotted as a function of Reynolds number both for axisymmetric and for nonaxisymmetric perturbations.

The perturbation resulting in the greatest instantaneous energy growth rate can be found as discussed earlier from eigenanalysis of $[(\boldsymbol{M}^{1/2}\boldsymbol{T}\boldsymbol{M}^{-1/2})^\dagger + \boldsymbol{M}^{1/2}\boldsymbol{T}\boldsymbol{M}^{-1/2}]/2$, from which the critical Reynolds number R_m^c beyond which there can be no growth can be determined. For the considered flow and for axisymmetric perturbations and axial wavenumber $k = -1$ it is found that there cannot be any perturbation growth for approximately $R_m < 200$. For higher

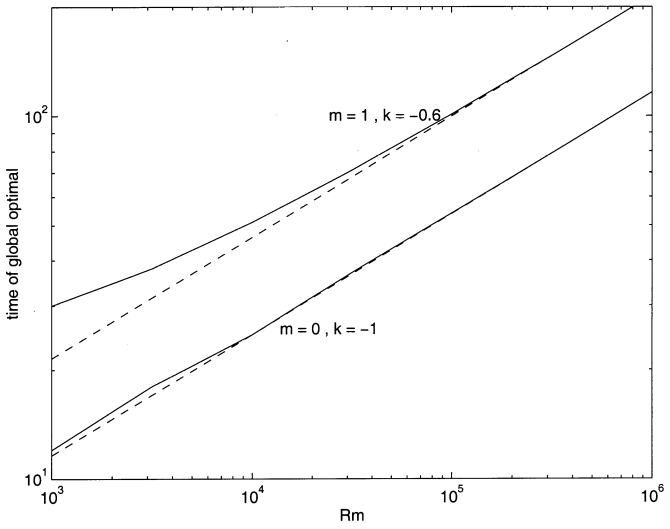

FIG. 9.—Time at which the global optimal energy is attained as a function of R_m for azimuthal and axial wavenumbers $m = 1$, $k = -0.6$ and $m = 0$, $k = -1$. The dashed lines correspond to $R_m^{1/3}$.

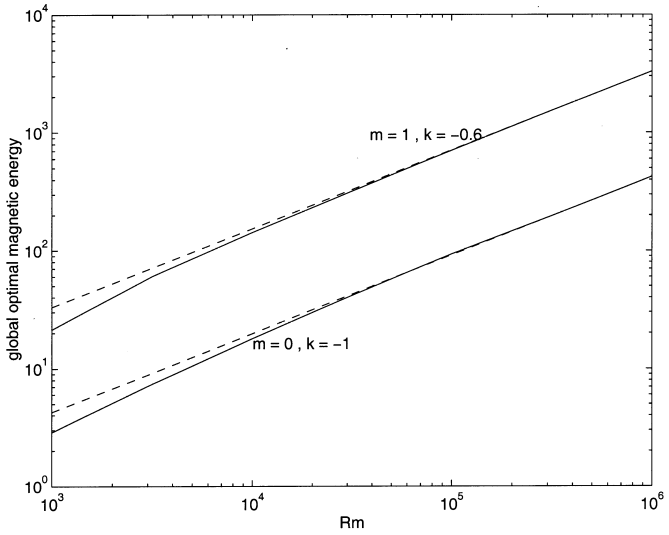

FIG. 10.—Global optimal energy growth for azimuthal and axial wavenumbers $m = 1$, $k = -0.6$ and $m = 0$, $k = -1$ as a function of R_m. The dashed lines correspond to $R_m^{2/3}$.

Reynolds number the instantaneous growth rate quickly approaches asympotically the inviscid maximum instantaneous growth rate, which is found to be 0.13.

4. DISCUSSION AND CONCLUSIONS

Stellar and galactic bodies commonly contain magnetic fields embedded in moving conducting fluids. In the physical circumstances addressed in this work these magnetic fields are sufficiently weak that Lorentz forces can be ignored in the momentum equation of the fluid motions, and in these cases the induction equation that describes the evolution of the magnetic field is explicitly linear. However, while linear, the induction equation is generally nonnormal, owing to the straining field of the moving conductor. These fluid motions organize and amplify the magnetic fields in the conducting fluid, producing coherent large-scale field structures. A traditional method for analyzing this process of growth and emergence of structure in conducting fluids is modal stability analysis, which has been extensively applied to the induction equation in connection with study of the initiation of a self-sustained dynamo. However, magnetic field growth is not confined to fields of modal form, and it has been previously noted that transient field growth arising from nonmodal processes must be included in a comprehensive stability analysis of the induction equation.

In this work a systematic analysis of nonmodal field growth has been presented. This generalized stability analysis allows identification of optimally growing field structures and places constructive limits on field growth. The generalized stability analysis presented here subsumes modal stability analysis, and unlike modal stability analysis can be extended to address also the stability properties of aperiodic nonautonomous operators (Farrell & Ioannou 1996b).

The helical dynamo of Lortz was chosen as a canonical example to illustrate application of generalized stability analysis to the induction equation. Transient growth in magnetic field increasing with magnetic Reynolds number is found over a large region in parameter space. This contrasts with the results of a modal stability analysis of the same model problem, which show instability confined to a small region in parameter space and modal growth rates decreasing with R_m, indicative of a slow dynamo. Perturbations producing optimal energy growth at a given time have been identified for this problem, and in addition perturbations optimally exciting the modes have been identified for both growing and decaying modes. The structures producing optimal instantaneous growth provide a strict bound on the rate of increase of the magnetic field that can be extended to the time-dependent problem. For sufficiently high R_m the structure producing maximum excitation of a given mode grows at first by stretching and then inherits the large-scale structure of the mode even in cases for which the mode itself is stable.

These results demonstrate a mechanism for emergence of large-scale field structure from small perturbations in primordial galactic fields. By extension, continual forcing by internally generated or externally imposed fields combined with transient growth can sustain field structures the analysis of which involves stochastically forcing the underlying nonnormal dynamo system (Farrell & Ioannou 1999a).

This work was supported in part by NSF ATM-9216813.

APPENDIX A

MAGNETIC FIELD GROWTH IN CONSTANT SHEAR

Consider a local approximation of the azimuthal velocity by a Cartesian planar flow with a constant shear $\bar{u}(y) = \alpha y$, $\bar{u}$ being in the streamwise direction x with unit vector $\boldsymbol{i}$, and y being the cross-stream direction with unit vector $\boldsymbol{j}$. In such a

simplified situation the nondimensional equation for the vector potential A, which is related to the magnetic field by $\boldsymbol{B} = \nabla \wedge (A\boldsymbol{k})$, takes the form

$$\frac{\partial A}{\partial t} + \alpha y \frac{\partial A}{\partial x} = \frac{1}{R_m} \nabla^2 A \,. \tag{A1}$$

It is easy to show that initially sinusoidal perturbations $A(x, y, 0) = A_0 e^{i(kx + ly)}$ will evolve at time t to

$$A(x, y, t) = A_0 \exp \left\{ ik(x - \alpha y t) + ily - \frac{1}{R_m} \int_0^t d\tau [k^2 + (l - \alpha k \tau)^2] \right\}, \tag{A2}$$

showing that the effective diffusion coefficient in the presence of shear is

$$D = \frac{1}{t} \int_0^t d\tau \, \frac{k^2 + (l - \alpha k \tau)^2}{R_m} \,. \tag{A3}$$

Consequently, the diffusive effects become important at a time $cR_m^{1/3}$ with the constant being given by $c = (3/\alpha^2 k^2)^{1/3}$.

The energy growth of these plane-wave initial perturbations is easily found to be

$$\frac{E(t)}{E(0)} = \frac{1 + (m - \alpha t)^2}{1 + m^2} \, e^{-2Dt} \,, \tag{A4}$$

where $m = l/k$ is the slope of the lines of constant phase of the plane wave. Consequently the instantaneous energy growth rate, g, is given by

$$g = \frac{-2\alpha m}{1 + m^2} - \frac{2k^2}{R_m} (1 + m^2) \,, \tag{A5}$$

which is maximized by a plane wave that satisfies

$$m^2 = 1 + \frac{2k^2 m}{\alpha R_m} (1 + m^2)^2 \,. \tag{A6}$$

As the Reynolds number increases, a maximum instantaneous growth of $|\alpha| - 4k^2/R_m$ is achieved for plane waves with $m = -\text{sgn } \alpha + 4k^2/(\alpha R_m)$, i.e., as $R_m \to \infty$ the perturbation is aligned with the direction of maximum stretching, which for a constant shear flow lies at 45° from the direction of the flow. The maximum instantaneous magnetic field stretching of fields aligned in this direction produces maximum instantaneous growth rate of the magnetic field.[3] As the magnetic Reynolds number decreases, the greatest initial growth rate also decreases until the critical Reynolds number $R_m^c = 16\sqrt{3}\, k^2/(9|\alpha|)$ for which no growth is possible is reached. The plane wave associated with this critical Reynolds number lies at 60° from the direction of flow. For $R_m < R_m^c$ no growth is possible.

[3] This result contrasts with the transient energy growth of stream function perturbations in two-dimensional constant shear flow in which, according to inviscid dynamics, energy is given by the reciprocal of eq. (A4) and the stream function with maximum instantaneous growth rate has wavenumber $m = \text{sgn } \alpha$, i.e., in the direction of maximum compression, which lies at 135° from the direction of the flow.

REFERENCES

Braginskii, S. I. 1965a, Soviet Phys.—JETP, 20, 726
———. 1965b, Soviet Phys.—JETP, 20, 1462
Butler, K. M., & Farrell, B. F. 1992, Phys. Fluids A, 4, 1637
Childress, S., & Gilbert, A. D. 1995, Stretch, Twist, Fold: The Fast Dynamo (New York: Springer)
Cowling, T. G. 1934, MNRAS, 94, 39
Farrell, B. F. 1982, J. Atmos. Sci., 39, 1663
———. 1984, J. Atmos. Sci., 41, 668
———. 1988, Phys. Fluids, 31, 2093
———. 1989, J. Atmos. Sci., 46, 1193
Farrell, B. F., & Ioannou, P. J. 1993a, J. Atmos. Sci., 50, 200
———. 1993b, Phys. Fluids A, 5, 1390
———. 1996a, J. Atmos. Sci., 53, 2025
———. 1996b, J. Atmos. Sci., 53, 2041
———. 1999a, ApJ, 522, 1088
———. 1999b, J. Atmos. Sci., in press
Gilbert, A. D. 1988, Geophys. Astrophys. Fluid Dyn., 44, 214
Gubbins, D. 1973, Phil. Trans. R. Soc. A. 274, 493
Gustavsson, L. H. 1991, J. Fluid Mech., 224, 241
Hoyng, P. 1987a, A&A, 171, 348
———. 1987b, A&A, 171, 357
———. 1988, ApJ, 332, 857
Hoyng, P. 1992, The Sun: A Laboratory for Astrophysics, ed J. T. Schmelz & J. C. Brown (Dordrecht: Kluwer), 1
Howard, A. M., & Kulsrud, R. M. 1997, ApJ, 483, 648
Kelvin, Lord. 1887, Phil. Mag., 24, 188
Krause, F., & Rädler, K.-H. 1980, Mean Field Magnetohydrodynamics and Dynamo Theory (London: Pergamon)
Lortz, D. 1968, Plasma Phys., 10, 967
Moffatt, H. K. 1978, Magnetic Field Generation by Electrically Conducting Fluids (Cambridge: Cambridge Univ. Press)
Orr, W. McF. 1907, Proc. R. Irish Acad., 27, 9
Parker, E. N. 1963, ApJ, 138, 552
Pekeris, C. L., Accad, Y., & Shkoller, B. 1973, Phil. Trans. R. Soc. A, 275, 425
Reddy, S. C., & Henningson, D. S. 1993, J. Fluid Mech., 252, 209
Ruzmaikin, A. A., Sokoloff, D. D., & Shukurov, A. M. 1988, J. Fluid Mech., 197, 39
Trefethen, L. N., Trefethen, A. E., Reddy, S. C., & Driscoll, T. A. 1993, Science, 261, 578
Tung, K.-K., 1983, J. Fluid Mech., 133, 443
Zeldovich, Ya. B., Ruzmaikin, A. A., & Sokoloff, D. D. 1983, Magnetic Fields in Astrophysics (New York: Gordon & Breach)